

# Synthesis, Characterization and Biological Activity Study of a New Schiff Base-Oxime Derived Ligand and Its Complexes with Some Metal Ions

Mahmood R. Mahmood<sup>1</sup>, Abdul Salam A K. Abdul Rahman<sup>2</sup>, Nasry Jassim Hussien<sup>2</sup>,  
Baydaa Muhi Nsaif<sup>2</sup>, Maha A Mahmood<sup>2</sup> and Siti Fairus Mohd Yusoff<sup>3</sup>

<sup>1</sup> Chemistry teacher, Ministry of Education, 00964 Baquba, Iraqi

<sup>2</sup>Department of Chemistry, College of Education for Pure Sciences, University of Diyala, 32001 Baqubah, Diyala, Iraq

<sup>3</sup>School of Chemical Sciences and Food Technology, Faculty of Science and Technology, Universiti Kebangsaan Malaysia, 43600 UKM Bangi, Selangor, Malaysia

mahmoodrafid3@gmail.com, nasry.hussien@uodiyala.edu.iq

**Keywords:** Oxime, Imine, Schiff Base, Complexes, Azomethine.

**Abstract:** A new ligand, (3Z)-3-((2-amino-4,5-dimethylphenyl)imino)butan-2-one oxime (L), was created in this research by combining 4,5-dimethyl-1,2-phenylenediamine with diacetyl monooxime in boiling CCl<sub>4</sub>. The ligand's structure was confirmed using elemental analysis and various spectroscopic techniques including FT-IR, UV, <sup>1</sup>H NMR, <sup>13</sup>C NMR, and mass spectrometry. Co(II), Ni(II), Cu(II), and Zn(II) metal ions were complexed with a specific ligand by reacting their chloride salts with the ligand in methanol at a 1:1 molar ratio under reflux conditions. The complexes' structure was confirmed using elemental analysis, spectroscopic methods, magnetic moments, and molar conductivity investigations. The complexes exhibited tetrahedral, square planar, and octahedral geometries for Zn(II), Ni(II), Co(II), Cu(II), and, respectively. In addition to all that has been mentioned, We also obtained the biological activity of the prepared compounds against Gram-positive bacteria (*Staphylococcus aureus*) and Gram-negative bacteria (*Escherichia coli*) at different concentrations of the ligand and the prepared complexes. It was found that some of them were effective at certain concentrations, while others were not effective. In addition, the effectiveness of the cobalt complex with bacteria was examined in the presence of the antibiotic (Levofloxacin), and it was found to be effective.

## 1 INTRODUCTION

Hugo Schiff, a German scientist, coined the term "Schiff base" in 1864 to characterize the compounds resulting from the combination of primary amines with carbonyl compounds. Despite originating over a decade before the establishment of coordination chemistry, Schiff bases continue to hold significance as ligands. They represent a vital category of compounds distinguished by the presence of a double bond (-C=N-) between carbon and nitrogen atoms [1]. These compounds exhibit various noteworthy attributes, such as high thermal stability, flame retardancy, and degradability. As a result, they have been widely employed in catalyst development, gas separation, and drug release industries [2]. Schiff bases stand out as among the most extensively utilized organic compounds, showcasing a diverse array of biological activities. These include but are not limited to antifungal, antibacterial, antimalarial, antiproliferative, anti-inflammatory, antiviral, and antipyretic properties [3]. Oximes and their derivatives are important bioactive ligands widely used in coordination chemistry. Oximes

are formed through the condensation of hydroxylamine with aldehydes or ketones. The oxime functional group exhibits amphoteric properties, with the azomethine group's nitrogen (C=N) being slightly basic and the hydroxyl group (OH) slightly acidic [4]. Advancements in both inorganic and bioinorganic chemistry have sparked greater interest in Schiff base complexes. This is driven by the recognition that numerous such complexes can potentially serve as models for emulating biomolecules [5]. Imine-oxime ligands have played a crucial role in coordination chemistry, exhibiting distinct chelation behaviours. They find various applications in analytical chemistry, including metal ion extraction and spectrophotometric determination. Moreover, certain imine-oxime complexes have been employed in catalyzing numerous organic reactions [6]. The biological activity of these compounds is frequently linked to their capacity to form complexes with the metals found in biosystems [7]. Additionally, certain hydrazones and oximes have found applications as herbicides, insecticides, nematocides, rodenticides, and plant growth regulators. They are also utilized as plasticizers and

stabilizers for polymers [8]. In addition, they play a significant role in applications in the fields of medicine, industry, and analysis [9]. The number of amine-imine-oxime complexes that have been reported is very low, even though a significant number of oximes and associated transition metal ion complexes have been investigated [10].

## 2 MATERIALS, METHODS, AND EXPERIMENTAL TECHNIQUES

### 2.1 Chemicals and Reagents

The synthetic work was carried out exclusively with analytical-grade substances. Among the main reagents employed were diacetyl monoxime (99%, Merck, Germany) and 4,5-dimethyl-1,2-phenylenediamine (97%, Sigma, USA). Additional salts included cesium iodide (98%, Merck, Germany), cobalt(II) chloride hexahydrate, copper(II) chloride dihydrate, nickel(II) chloride hexahydrate, and zinc(II) chloride (all  $\geq 99\%$ , Sigma, USA). Methanol of 99% purity (Merck, Germany) was used as the principal solvent.

### 2.2 Analytical and Spectroscopic Characterization

To ensure proper identification of the obtained products, a series of instrumental methods was applied. Elemental analyses (C, H, N) were performed with an Eager 300 (EA112). Infrared spectra were obtained on a SHIMADZU 8400S spectrophotometer, applying both KBr and CsI pellets. Proton and carbon NMR ( $^1\text{H}$  and  $^{13}\text{C}$ ) were measured on a Bruker 400 MHz instrument. UV-Vis spectra were registered using quartz cuvettes of 1 cm path length. The magnetic properties of the complexes were evaluated at room temperature with a Sherwood Scientific balance. Molar conductance was measured on a Starter 3000°C conductivity meter [11].

### 2.3 Synthetic Strategy

#### 2.3.1 Ligand Preparation

The ligand (3Z)-3-((2-amino-4,5-dimethylphenyl)imino)butan-2-one oxime (L) was obtained by condensation of 4,5-dimethyl-1,2-phenylenediamine (2.1 g, 15 mmol) with diacetylmonoxime (1.55 g, 15 mmol) in carbon tetrachloride (15 mL). The reaction was maintained under reflux with continuous stirring for 3 h. During the course of the process, the solution initially appeared dark brown and later produced a light creamy solid. The precipitate was isolated by filtration, washed sequentially with  $\text{CCl}_4$

(5 mL) and cold ethanol (3 mL), and finally dried. Yield: 1.6 g (50%); colour: creamy; m.p.: 130–134 °C.

#### 2.3.2 Synthesis of Metal Complexes

Complexes were synthesized by reacting the ligand with the respective metal salts in methanolic solution:

- [L  $\text{ZnCl}$ ]Cl (C1): Ligand L (0.3 g, 1 mmol) in 10 mL methanol was mixed with  $\text{ZnCl}_2$  (0.136 g, 1 mmol) dissolved in 5 mL methanol. The mixture was refluxed at 95 °C for 3 h. A light green solid was obtained after cooling and filtration. Yield: 0.2 g (57%); m.p.: 200–206 °C.
- [L  $\text{CoCl}(\text{H}_2\text{O})_2$ ]Cl (C2): Prepared analogously, substituting cobalt(II) chloride hexahydrate (0.237 g, 1 mmol) for zinc chloride. The obtained product was dark green. Yield: 0.26 g (76.4%); m.p.: 183–185 °C.
- [L  $\text{CuCl}(\text{H}_2\text{O})_2$ ]Cl (C3): Using copper(II) chloride dihydrate (0.17 g, 1 mmol), a dark green solid was isolated. Yield: 0.23 g (67.6%); m.p.: 155–160 °C.
- [L  $\text{NiCl}_2$ ] (C4): Reaction with nickel(II) chloride hexahydrate (0.23 g, 1 mmol) afforded a red compound. Yield: 0.22 g (64.7%); m.p.: 266–270 °C.

### 2.4 Antibacterial Screening

The newly obtained compounds were subjected to antimicrobial tests against *Escherichia coli* and *Staphylococcus aureus*. A disc diffusion method was applied. Three concentrations were prepared: 100  $\mu\text{g/mL}$  (stock), 50  $\mu\text{g/mL}$  (diluted in DMSO), and 25  $\mu\text{g/mL}$ . The inhibitory effects were evaluated after incubation.

### 2.5 Culture Medium Preparation

Mueller–Hinton agar was prepared by dissolving 38 g of the medium in 1 L of distilled water, sterilized by autoclaving at 121 °C and 15 psi for 15 min. Once cooled, it was poured into sterile Petri dishes and stored under refrigeration. During testing, 100  $\mu\text{L}$  of each compound solution was applied into wells, with sterile distilled water used as positive and negative controls. Incubation was carried out at 37 °C for 24 h [12], [13].

## 3 RESULT AND DISCUSSION

### 3.1 Synthesis and Characterization of the Ligand and Complexes

The Schiff base–oxime ligand (L) was obtained via condensation of diacetylmonoxime with 4,5-dimethyl-o-

phenylenediamine (Fig. 1). Its elemental analysis data matched well with the theoretically calculated values (Table 1), confirming the proposed molecular formula. Structural verification was additionally supported by a combination of spectroscopic techniques, including IR, UV-Vis,  $^1\text{H}$  and  $^{13}\text{C}$  NMR, and EI-MS. Complexes of L with Co(II), Cu(II), Ni(II), and Zn(II) were synthesized

through reactions of the ligand with the corresponding hydrated metal chlorides in methanol at reflux, maintaining a 1:1 molar ratio (Fig. 2). The microanalytical and metal content results for all complexes (Table 1) further confirmed their compositions.

Table 1: Elemental analyses data and physical properties of ligands and their complexes.

No	Molecular Formula	M.wt g/mol	Yield%	Colour	m.p $^{\circ}\text{C}$
L	$\text{C}_{12}\text{H}_{17}\text{N}_3\text{O}$	219.2	50%	Creamy	130-136
C <sub>1</sub>	$\text{C}_{12}\text{H}_{17}\text{Cl}_2\text{ZnN}_3\text{O}$	355.5	57%	light green	200-206
C <sub>2</sub>	$\text{C}_{12}\text{H}_{21}\text{Cl}_2\text{CoN}_3\text{O}_3$	385.1	76.4%	Dark green	183-185
C <sub>3</sub>	$\text{C}_{12}\text{H}_{21}\text{Cl}_2\text{CuN}_3\text{O}_3$	389.7	67.6%	Dark green	155-160
C <sub>4</sub>	$\text{C}_{12}\text{H}_{17}\text{Cl}_2\text{NiN}_3\text{O}$	348.8	64.7%	Red	266-270

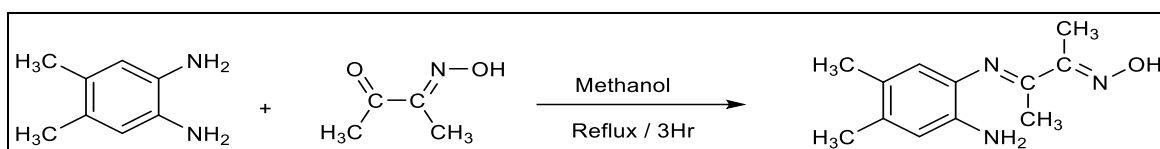


Figure 1: Preparation route of the ligands.

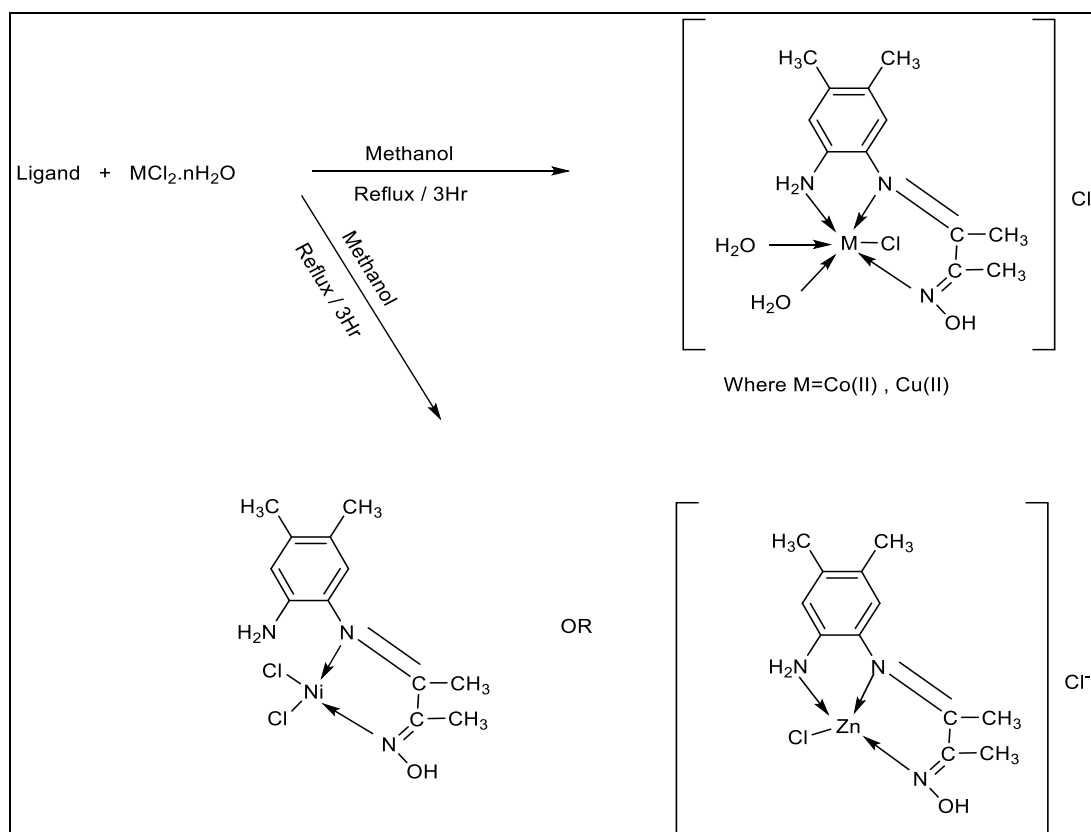


Figure 2: Preparation route of the Complexes.

### 3.2 Infrared Spectroscopy

The IR spectrum of ligand L displayed several diagnostic bands:  $\nu(\text{NH})$  stretching at 3379 and 3155  $\text{cm}^{-1}$ ,  $\nu(\text{OH})$  of the oxime group at 3286  $\text{cm}^{-1}$ , and  $\nu(\text{C}=\text{N})$  of imine and oxime at 1627 and 1581  $\text{cm}^{-1}$ , respectively. Upon complexation, the  $\nu(\text{C}=\text{N})$  signals shifted to lower frequencies ( $\sim 1573$   $\text{cm}^{-1}$ ), reflecting coordination of the azomethine and oxime nitrogens with the metal centers. The  $\nu(\text{N}-\text{O})$  band of the free ligand at 1134  $\text{cm}^{-1}$  shifted to 1165–1265  $\text{cm}^{-1}$  in the complexes, also supporting

metal–ligand bonding. New absorptions at 475–425  $\text{cm}^{-1}$  and 300–246  $\text{cm}^{-1}$  were observed in all complexes, assignable to  $\nu(\text{M}-\text{N})$  and  $\nu(\text{M}-\text{Cl})$ , respectively, and were absent in the free ligand spectrum [14], [15]. Additionally, the spectra of Co(II) and Cu(II) complexes showed features due to coordinated water molecules (e.g., 609, 1774, 3518  $\text{cm}^{-1}$  for LCo; 864, 1797  $\text{cm}^{-1}$  for LCu). (Fig. 3-4, Table 2).

Table 2: Infrared spectra for ligands and their complexes

No	$\nu(\text{N}-\text{H})$ Assm. Ssm.	$\nu(\text{C}=\text{N})$ Imine	$\nu(\text{C}=\text{N})$ Oxime	$\nu(\text{N}-\text{O})$	$\nu(\text{M}-\text{N})$	$\nu(\text{M}-\text{Cl})$
L <sup>1</sup>	3379m 3155m	1627s	1581m	1134m	-----	-----
C <sub>1</sub>	3270m 3170w	1573m	1458m	1165m	475w	246m
C <sub>2</sub>	3170w	1573w	1381w	1226m	439w	300w
C <sub>3</sub>	3194 3156	1627	1404	1265w	432w	262w
C <sub>4</sub>	3170w	1573s	1442w.b	1242m	425w	250w

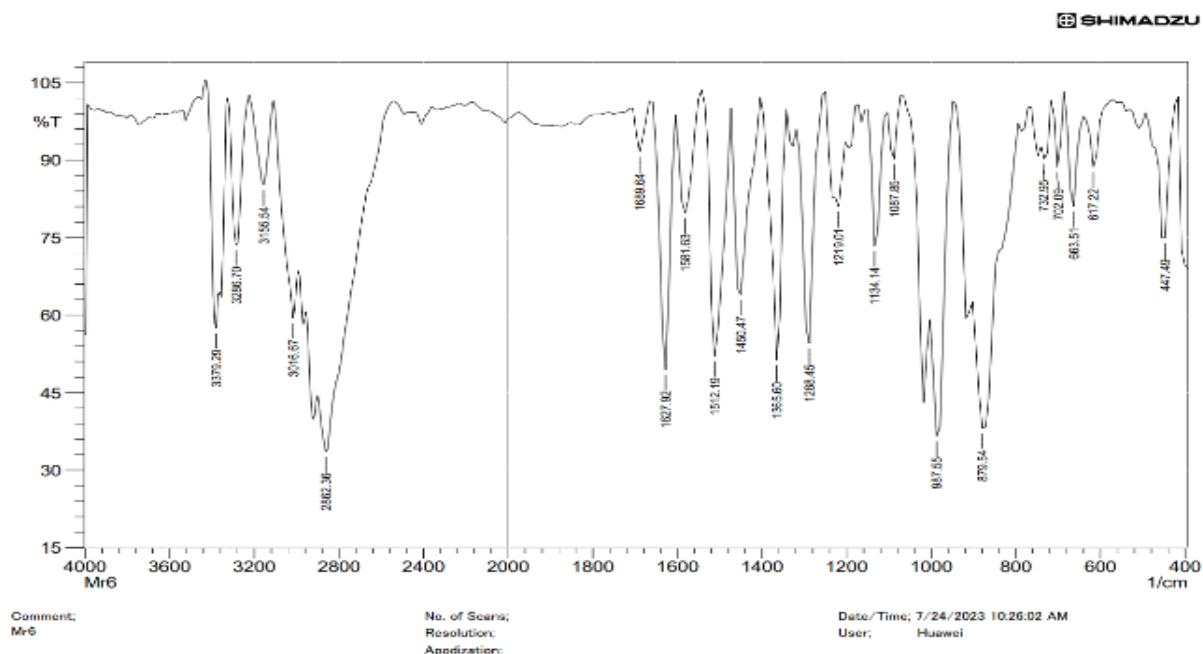


Figure 3: FT – IR spectrum of the Ligand.

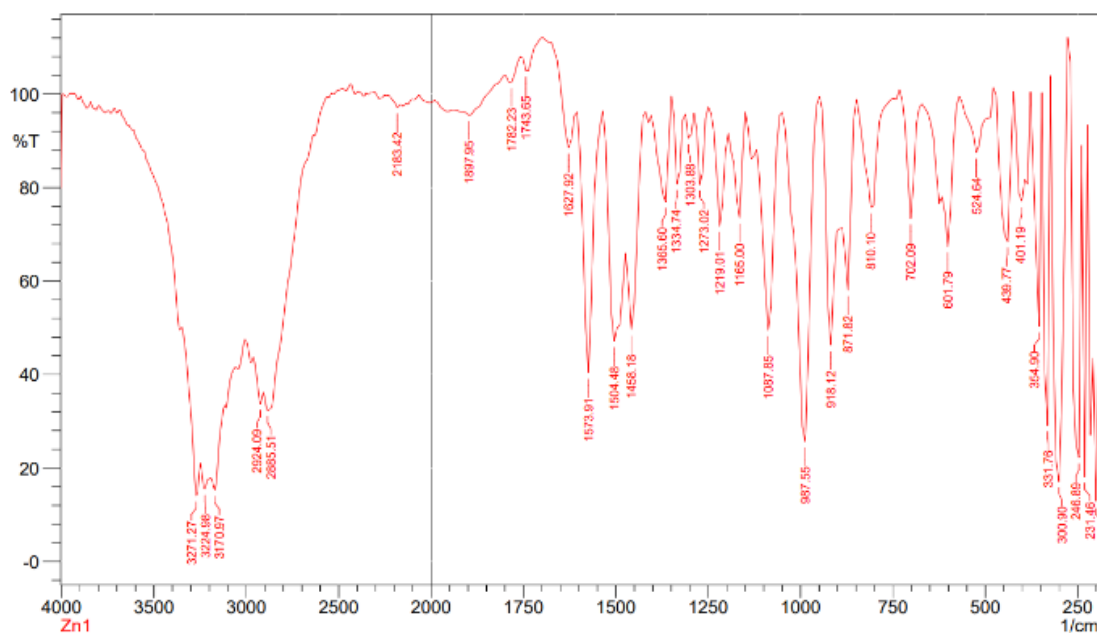


Figure 4: FT – IR spectrum of the [L ZnCl] Cl complex.

### 3.3 Electronic Absorption Spectra

The UV–Vis spectrum of the free ligand (Fig. 5) exhibited a strong band at 314 nm ( $31,847\text{ cm}^{-1}$ ,  $\epsilon = 1265\text{ L}\cdot\text{mol}^{-1}\cdot\text{cm}^{-1}$ ), attributed to  $\pi\rightarrow\pi^*$  and  $n\rightarrow\pi^*$  transitions. In the LCu complex, a ligand-centered transition appeared at 258 nm ( $38,760\text{ cm}^{-1}$ ), accompanied by a charge-transfer band at 364 nm. Weak d–d transitions at 662 and 930 nm were consistent with an octahedral geometry around Cu(II) [2], [16]. The LCo complex (Fig. 6) displayed intense bands at 256 and 272 nm ( $\pi\rightarrow\pi^*$  and  $n\rightarrow\pi^*$ ) along with a charge transfer peak at 320 nm. A weak absorption at 500 nm was assigned to the  $^4\text{T}_{1g} \rightarrow ^4\text{A}_{2g}$  transition, also supporting an octahedral environment [17], [18].

For LNi, the spectrum showed  $\pi\rightarrow\pi^*$  and  $n\rightarrow\pi^*$  bands at 324 nm ( $30,864\text{ cm}^{-1}$ ), while additional absorptions at 564 and 644 nm corresponded to  $^1\text{A}_{1g} \rightarrow ^1\text{B}_{1g}$  and  $^1\text{A}_{1g} \rightarrow ^1\text{A}_{2g}$  transitions, consistent with a square-planar geometry [18], [19]. In the LZn spectrum, intense absorptions at 256 and 318 nm were characteristic of ligand-centered and charge transfer transitions typical for tetrahedral Zn(II) complexes [17], [19]. Full spectral data are summarized in Table 3.

### 3.4 Conductivity and Magnetic Properties

Molar conductivity values ( $43\text{--}65\text{ S}\cdot\text{cm}^2\cdot\text{mol}^{-1}$ ) indicated that all complexes, except LNi, behaved as 1:1 electrolytes in solution, while Ni(II) complex was non-

electrolytic [20] (Table 4). Magnetic moment measurements (Table 5) supported the proposed geometries: octahedral for Co(II) and Cu(II) ( $\mu_{\text{eff}} = 2.19\text{ BM}$ ), square planar for Ni(II) ( $\mu_{\text{eff}} = 0.7\text{ BM}$ ), and tetrahedral for Zn(II). These results are consistent with the spectral analyses [21].

### 3.5 NMR Spectroscopy

The  $^1\text{H}$  NMR spectrum of ligand L in DMSO- $d_6$  (Fig. 7) displayed a diagnostic oxime proton at 11.40 ppm (singlet), which disappeared upon  $\text{D}_2\text{O}$  exchange. Aromatic and  $\text{NH}_2$  protons resonated between 6.49–6.30 ppm, with  $\text{NH}_2$  also vanishing after  $\text{D}_2\text{O}$  addition. Methyl groups were observed at 1.96, 2.29, and 2.63 ppm. In the LZn complex, these resonances shifted significantly: the  $\text{NH}_2$  protons appeared at 4.24 ppm, and the oxime proton at 11.39 ppm, confirming coordination. The aromatic signals were shifted downfield, and methyl resonances appeared at 1.97, 2.40, and 2.61 ppm (Table 6).

The  $^{13}\text{C}$  NMR spectrum of L (Fig. 8) revealed signals for  $\text{C}=\text{N}-\text{OH}$  at 164.78 ppm and  $\text{C}=\text{N}-$  at 153.49 ppm, along with aromatic carbons between 137–166 ppm. Methyl carbons appeared at 23.12, 20.21, 19.58, and 9.81 ppm [22]–[25]. In LZn, the oxime carbon signal shifted downfield to 153.16 ppm, confirming metal coordination. Other carbons showed comparable but slightly shifted signals (Table 7) [28].

Table 3: Electronic spectral data of L1 and its metal complexes.

No	$\lambda$ nm	$\lambda$ $\text{cm}^{-1}$	$\Sigma\text{Max}$ ( $\text{dm}^3 \text{ mol}^{-1} \text{ cm}^{-1}$ )	Assignment	Suggested geometry
L <sup>1</sup>	314	31847	1265	Ligand Field	-----
C <sub>1</sub>	256 318 372	39063 31447 26882	1796 1500 95	Ligand Field Charge transfer Charge transfer	Tetrahedral
C <sub>2</sub>	256 272 320 500	39063 36765 31250 20000	1441 1114 673 130	Ligand Field Ligand Field Charge transfer ${}^4\text{T}_{1(\text{g})} \text{F} \rightarrow {}^4\text{A}_{2(\text{g})} \text{F}$	Octahedral
C <sub>3</sub>	258 364 430 662 930	38760 27473 23256 15106 10753	2829 604 244 273 137	Ligand Field Charge transfer Charge transfer ${}^2\text{B}_{2(\text{g})} \rightarrow {}^2\text{B}_{1(\text{g})}$ ${}^2\text{B}_{2(\text{g})} \rightarrow {}^2\text{A}_{1(\text{g})}$	Octahedral
C <sub>4</sub>	324 564 644	30864 17731 15530	1604 250 164	Charge transfer ${}^1\text{A}_{1(\text{g})} \rightarrow {}^1\text{B}_{1(\text{g})}$ ${}^1\text{A}_{1(\text{g})} \rightarrow {}^1\text{A}_{2(\text{g})}$	Square planar

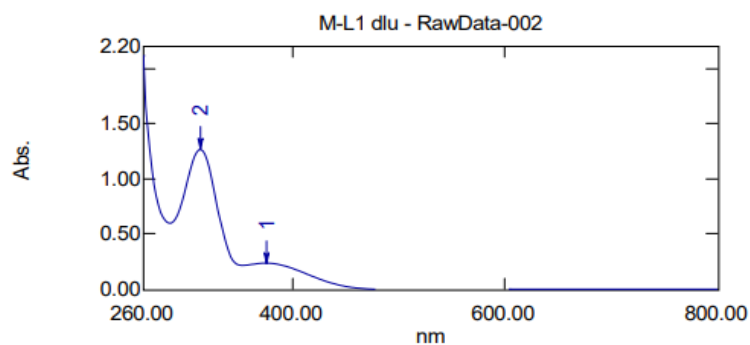


Figure 5: UV-VIS spectrum of the ligand.

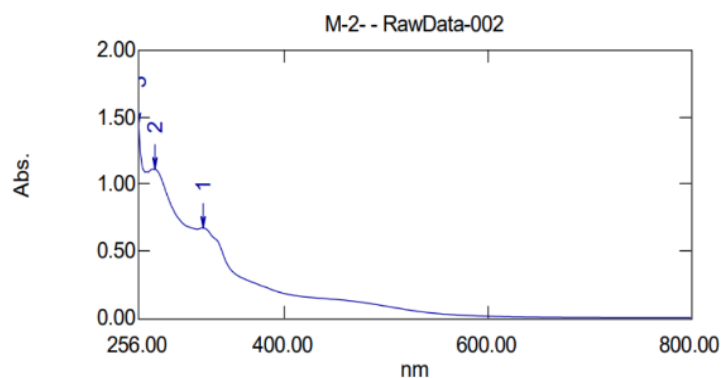

 Figure 6: UV-VIS spectrum of the LCoCl (H<sub>2</sub>O)<sub>2</sub>]Cl complex.

Table 4: The molar conductance of the complexes.

COMP.	COMPLEX	Molar conductivity S.cm <sup>2</sup> .mole <sup>-1</sup> Λ
C <sub>1</sub>	[LZnCl]Cl	43
C <sub>2</sub>	[LCoCl (H <sub>2</sub> O) <sub>2</sub> ]Cl	65
C <sub>3</sub>	[LCuCl (H <sub>2</sub> O) <sub>2</sub> ]Cl	136
C <sub>4</sub>	LNiCl <sub>2</sub>	43

 Table 5: Magnetic Moment ( $\mu_{\text{eff}}$  =B.M) of L1 complexes at 298K and suggested stereochemical structures.

Compound	$\mu_{\text{eff}}$ . B.M	Proposed Geometry
[LZnCl] Cl	diamagnetic	tetrahedral
[LCoCl (H <sub>2</sub> O) <sub>2</sub> ] Cl	2.19	octahedral
[LCuCl (H <sub>2</sub> O) <sub>2</sub> ] Cl	2.19	octahedral
LNiCl <sub>2</sub>	0.7	Square planar

 Table 6: <sup>1</sup>HNMR data ( $\delta$ , ppm) for the L1 ligand and L1Zn complex in DMSO-d<sub>6</sub>.

Funct. Group	$\delta$ (ppm) ( Ligand)	$\delta$ (ppm) ( C <sub>1</sub> )
-C=N-OH	11.40 (s,1H)	11.39 (s, 1H)
C-H (ar)	(6.30-6.49) (d,2H)	(6.32-7.93) (d, 2H)
CH <sub>3</sub> -C=N-OH	2.63 (s,3H)	2.61 (s, 3H)
CH <sub>3</sub> -C=N-	1.97(s,3H).	2.40(s, 3H).
CH <sub>3</sub> -C (ar)	2.29 (s,6H)	1.97 (d, 6H)
NH <sub>2</sub>	4.24 (s,2H)	4.24 (s, 2H)

 Table 7: <sup>13</sup>C nmr data for the ligand and L1Zn complex.

Funct. Group	$\delta$ (ppm) Ligand	$\delta$ (ppm) (C <sub>1</sub> ) Complex
-C <sub>9</sub> =N-OH	163.92	152.28
C <sub>7</sub> =N-	152.25	151.94
C <sub>13</sub> ,C <sub>5</sub> ,C <sub>4</sub> ,C <sub>16</sub> ,C <sub>15</sub> ,C <sub>14</sub> (ar)	(115.35-136)	(116.27-138.54)
C <sub>10</sub>	21.88	21.90
C <sub>1</sub>	18.97	18,99
C <sub>2</sub>	18.34	17.88
C <sub>8</sub>	8.56	8.59

Table 8: EI mass spectral data of L1 ligand.

Mass/charge m/z	Relative abundance
219	23
204	31
186	56
161	100
149	55
136	62
120	35
168	12
93	29
77.1	28
65	13
51	12

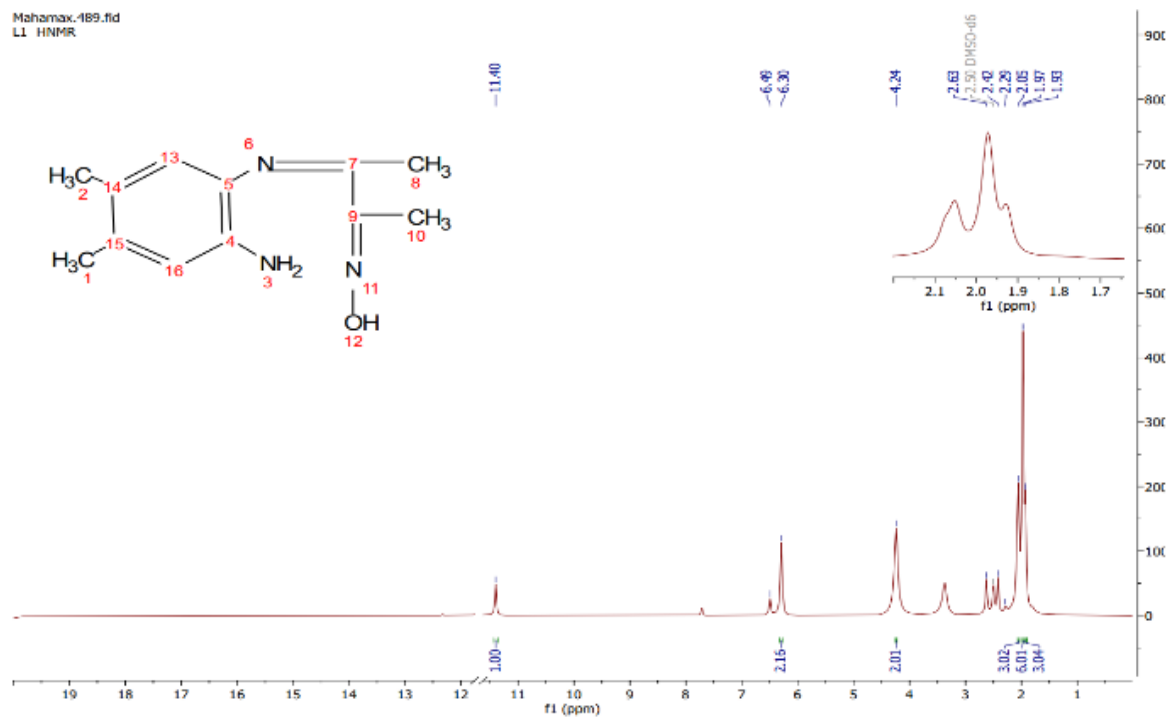


Figure 7: <sup>1</sup>Hnmr spectrum of the ligand.

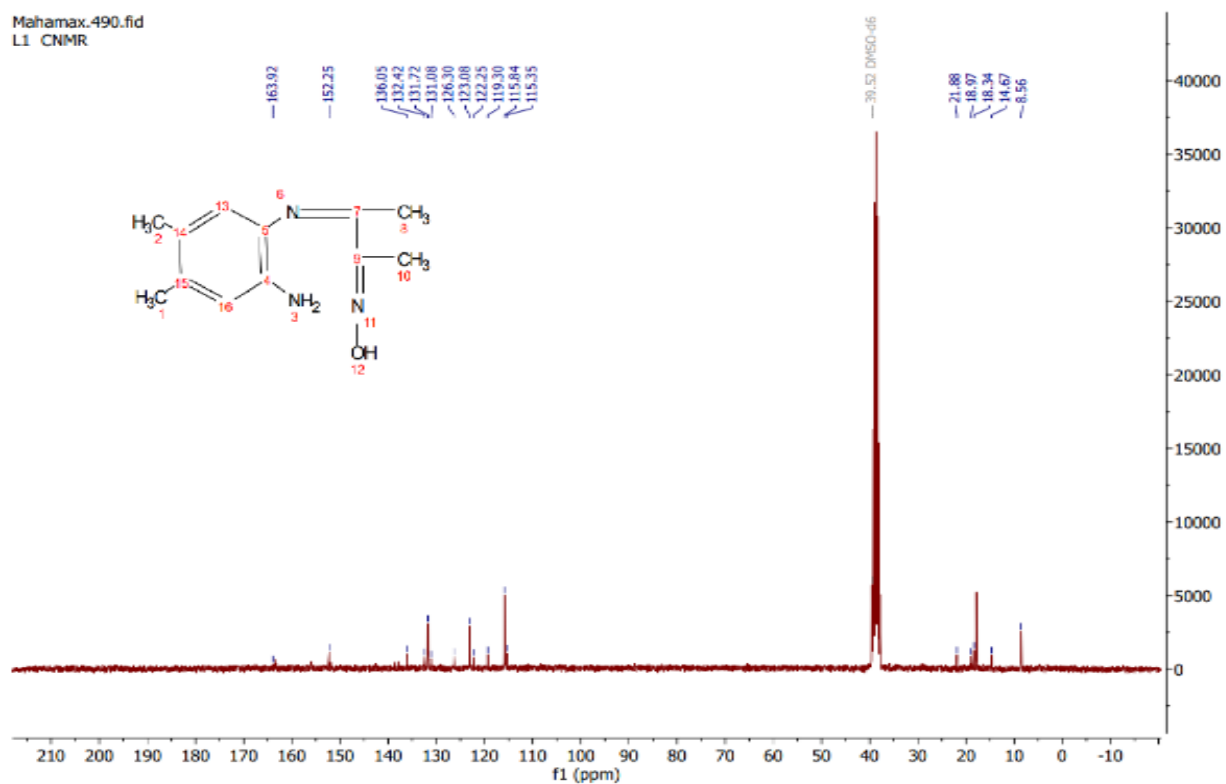


Figure 8: <sup>13</sup>Cnmr spectrum of the ligand.



Table 9: Biological activity and inhibition zone (mm) data for prepared ligand and their complexes.

Compound	Concentration, (µg/ml)	Staphylococcus Aureus, (G+)(mm)	Escherichia Coli, (G-)(mm)
L <sup>1</sup>	100	25	20
	50	17	16
	25	R	R
C <sub>1</sub>	100	18	17
	50	14	15
	25	R	R
C <sub>2</sub>	100	34	30
	50	25	20
	25	19	15
	Levofloxacin Control	23	26
		R	R
C <sub>3</sub>	100	21	18
	50	15	15
	25	13	14
C <sub>4</sub>	100	R	17
	50	R	15
	25	R	14

File :C:\MSDCHEM\1\DATA\Snapshot(L1).D  
 Operator :  
 Acquired : 29 Oct 2023 13:39 using AcqMethod default.m  
 Instrument : directmass  
 Sample Name:  
 Misc Info :  
 Vial Number: 1

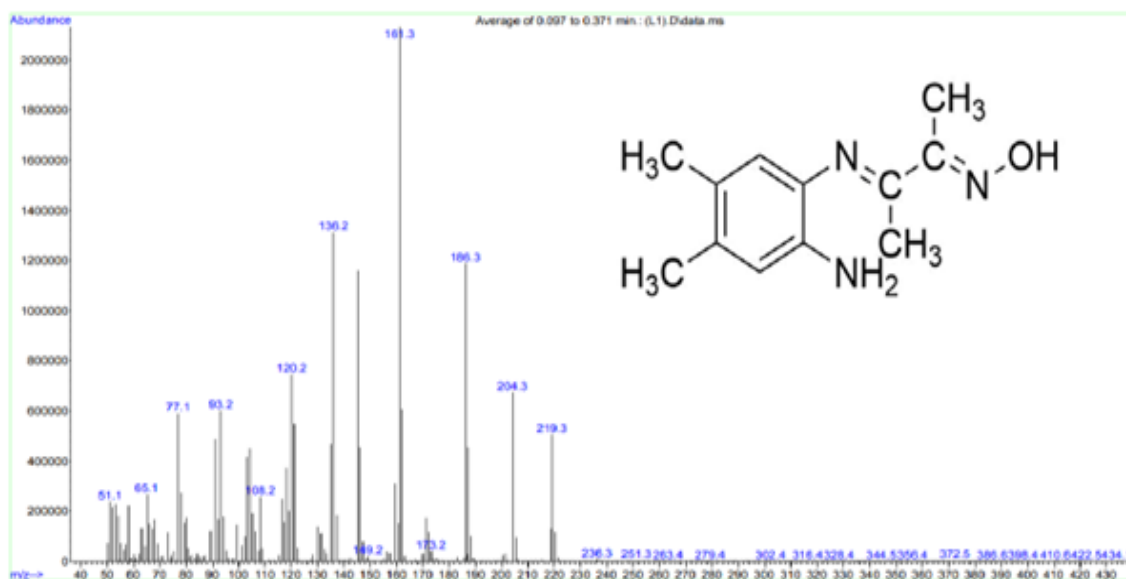


Figure 9: EI mass spectrum for the Ligand.

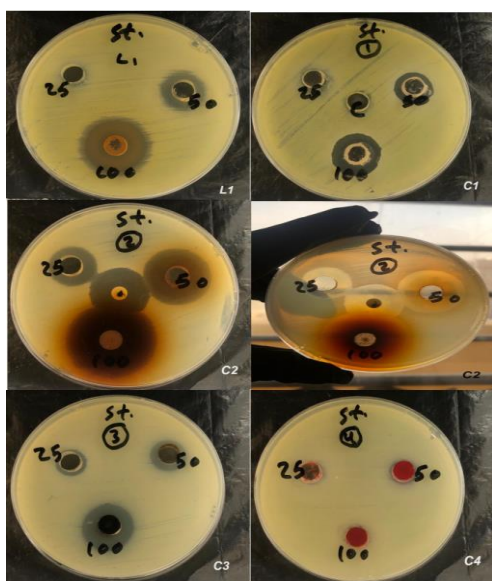


Figure 10. Evaluation of Antiviral Efficacy of the Ligand and Its Complexes [C1, C2, C3, C4] Against *Staphylococcus aureus*

### 3.6 Mass Spectrometry

The EI mass spectrum of the ligand displayed a molecular ion peak at  $m/z = 219$  ( $M^+$ ), matching the calculated molecular weight. Fragment ions are listed in Table 8 and illustrated in Figure 9. For LZn, the parent ion was observed at  $m/z = 355.57$ , again consistent with the expected formula.

### 3.7 Antibacterial Activity

The ligand and complexes were screened against *Staphylococcus aureus* (Gram-positive) and *Escherichia coli* (Gram-negative) at concentrations of 25, 50, and 100  $\mu\text{g/mL}$  in DMSO. At the lowest concentration (25  $\mu\text{g/mL}$ ), LZn and the free ligand exhibited no inhibitory effect against *S. aureus*, while LCo and LCu showed measurable activity. Similarly, against *E. coli*, both L and LZn were inactive at 25  $\mu\text{g/mL}$ , whereas all complexes except LNi were active at higher concentrations. Notably, the LNi complex showed no significant inhibition of *S. aureus* at any tested concentration (Table 9, Fig. 10) [29], [30].

## 4 CONCLUSIONS

Within the scope of this investigation, a novel Schiff base-oxime ligand was synthesized and characterized, in addition to its complexes with zinc ( $\text{Zn}^{2+}$ ), cobalt ( $\text{Co}^{2+}$ ), nickel ( $\text{Ni}^{2+}$ ), and copper ( $\text{Cu}^{2+}$ ), all of which were studied at reasonable relative ratios. Several methods, including magnetic susceptibility, molar conductivity, Fourier

transform infrared spectroscopy, nuclear magnetic resonance (NMR) with  $^{13}\text{C}$  and  $^1\text{H}$ , ultraviolet-visible spectroscopy, and mass spectroscopy, were utilized to investigate the complexes. Several of their structural characteristics were validated by the results that were obtained. The amine-oxime ligand and its metal complexes demonstrated activity that ranged from moderate to good against the two different species of bacteria that were utilized in this investigation. The geometric morphologies of the complexes were proposed, and the  $\text{Zn}^{2+}$  complex was found to be tetrahedral. On the other hand, the  $\text{Co}^{2+}$  and  $\text{Cu}^{2+}$  complexes were found to be octahedral, and the  $\text{Ni}^{2+}$  complex was found to be square planar. The article's principal objective is to catalyze ongoing study by providing readers with expansive insights into the astounding capabilities and multifarious complexity of the oxime moiety. This will be accomplished by providing readers with thorough information. Therefore, the continuous examination of these complexes may show to be a fruitful endeavour for future investigations. This prospect is supported by the fact that it is highly plausible.

## ACKNOWLEDGMENTS

The authors thank the Department of Chemistry, College of Education for Pure Sciences/ University of Diyala, for providing chemicals and support.

## REFERENCES

- [1] S. Kumar, P. Sekar, and S. K. Raju, "A Review on Microwave-Assisted Synthesis and Biomedical Applications of Schiff Bases."
- [2] O. A. Urucu, A. B. Çiğil, A. Zülfikaroğlu, and O. Esentürk, "UV-Curable Schiff Base-Containing Polymeric Adsorbent for Selective and Efficient Removal of Au (III) From Aqueous Solutions," *Materials Today Communications*, vol. 37, p. 107270, 2023.
- [3] A. Hamil, K. M. Khalifa, A. A. Almutaleb, and M. Q. Nouradean, "Synthesis, Characterization and Antibacterial Activity Studies of Some Transition Metal Chelates of Mn (II), Ni (II) and Cu (II) With Schiff Base Derived From Diacetylmonoxime With o-Phenylenediamine," *Adv. J. Chem. A*, vol. 3, no. 4, pp. 524-533, 2020.
- [4] Ü. Korkmaz, B. T. Findik, B. Dede, and F. Karipcin, "Synthesis, Structural Elucidation, In Vitro Antibacterial Activity, DFT Calculations, and Molecular Docking Aspects of Mixed-Ligand Complexes of a Novel Oxime and Phenylalanine," *Bioorganic Chemistry*, vol. 121, p. 105685, 2022.
- [5] Ş. Karadeniz, C. Y. Ataoğlu, T. Özen, R. Demir, H. Ögütçü, and H. Bati, "Synthesis, Characterization and Biological Activities of Ni (II), Cu (II) and UO<sub>2</sub> (VI) Complexes of N'-(2Z,3E)-3-(Hydroxyimino)butan-2-ylidene)-2-phenylacetohydrazide," *Journal of Molecular Structure*, vol. 1175, pp. 39-48, 2019.

- [6] A. H. Ismail, B. H. Al-Zaidi, and M. M. Hasson, "New Bidentate Schiff Base Complexes of Some Transition Ions: Preparation, Identification, With Studying the Antibacterial Behaviour," *Biochem. Cell. Arch.*, vol. 19, no. 1, pp. 1629-35, 2019.
- [7] V. M. Mounnissamy, J. Abdul, and E. Gangatharan, "Synthesis, Docking and Anti-Oxidant Activity of Zn (II) Complexes of Oximes," *World Journal of Pharmaceutical Sciences*, pp. 1650-1660, 2015.
- [8] Ş. Karadeniz, C. Y. Ataol, O. Şahin, Ö. İdil, and H. Bati, "Synthesis, Structural Studies and Antimicrobial Activity of N'-((2Z,3E)-3-(Hydroxyimino)butan-2-ylidene)-2-phenylacetohydrazide and Its Co (II), Ni (II) Complexes," *Journal of Molecular Structure*, vol. 1161, pp. 477-485, 2018.
- [9] T. Sardohan-Koseoglu, E. Kir, and B. Dede, "Preparation and Analytical Application of the Novel Hg (II)-Selective Membrane Electrodes Based on Oxime Compounds," *Journal of Colloid and Interface Science*, vol. 444, pp. 17-23, 2015.
- [10] E. Canpolat, A. Aglamis, H. Sahal, and M. Kaya, "Some Transition Metal Complexes of NO Type Schiff Base," *Preparation and Characterization: Science Journal (CSJ)*, vol. 37, pp. 1300-1949, 2016.
- [11] H. Liao, X. Lin, Y. Li, M. Qu, and Y. Tian, "Reclassification of the Taxonomic Framework of Orders Cellvibrionales, Oceanospirillales, Pseudomonadales, and Alteromonadales in Class Gammaproteobacteria Through Phylogenomic Tree Analysis," *mSystems*, vol. 5, no. 5, 2020, doi: 10.1128/mSystems.00543-20.
- [12] M. Balouiri, M. Sadiki, and S. K. Ibensouda, "Methods for In Vitro Evaluating Antimicrobial Activity: A Review," *Journal of Pharmaceutical Analysis*, vol. 6, no. 2, pp. 71-79, 2016.
- [13] A. Madani, Z. Esfandiari, P. Shoaee, and B. Ataei, "Evaluation of Virulence Factors, Antibiotic Resistance, and Biofilm Formation of Escherichia coli Isolated From Milk and Dairy Products in Isfahan, Iran," *Foods*, vol. 11, no. 7, p. 960, 2022.
- [14] D. Maity and D. Maity, "Cu (II) and Ni (II) Complexes of Schiff Base Ligands Derived From Diamines and Biacetyl Monoxime: A Review," *Jordan Journal of Chemistry (JJC)*, vol. 16, no. 3, pp. 105-121, 2021.
- [15] N. T. Dhokale and A. V. Nagawade, "Antimicrobial Studies on Novel Ni (II) Metal Complexes With Salicyloyl Pyrazole Oximes: Synthesis and Characterization," *Journal of Advanced Scientific Research*, vol. 11, no. 04, pp. 255-261, 2020.
- [16] P. Devi, K. Singh, B. Kumar, and J. K. Singh, "Synthesis, Spectroscopic, Antimicrobial and In Vitro Anticancer Activity of Co<sup>2+</sup>, Ni<sup>2+</sup>, Cu<sup>2+</sup> and Zn<sup>2+</sup> Metal Complexes With Novel Schiff Base," *Inorganic Chemistry Communications*, vol. 152, p. 110674, 2023.
- [17] S. Gozdas, M. Kose, V. McKee, M. Elmastas, I. Demirtas, and M. Kurtoglu, "Crystal Structures, Electronic Spectra and Anticancer Properties of New Azo-Azomethines and Their Nickel (II) and Copper (II) Chelates," *Journal of Molecular Structure*, vol. 1304, p. 137691, 2024.
- [18] S. Lebbouz, "The Synthesis and Evaluation of Antioxidant Activity of Schiff Bases Ligands: Investigation of Their Ion Extraction Capability From Aqueous Media," *Kasdi Merbah Ouargla University*.
- [19] T. Saritha and P. Metilda, "Synthesis, Spectroscopic Characterization and Biological Applications of Some Novel Schiff Base Transition Metal (II) Complexes Derived From Curcumin Moiety," *Journal of Saudi Chemical Society*, vol. 25, no. 6, p. 101245, 2021.
- [20] K. J. Al-Adilee, A. K. Abass, and A. M. Taher, "Synthesis of Some Transition Metal Complexes With New Heterocyclic Thiazolyl Azo Dye and Their Uses as Sensitizers in Photo Reactions," *Journal of Molecular Structure*, vol. 1108, pp. 378-397, 2016.
- [21] Y. M. Ahmed and G. G. Mohamed, "Synthesis, Spectral Characterization, Antimicrobial Evaluation and Molecular Docking Studies on New Metal Complexes of Novel Schiff Base Derived From 4,6-Dihydroxy-1,3-phenylenediethanone," *Journal of Molecular Structure*, vol. 1256, p. 132496, 2022.
- [22] S. Y. Uçan, "Synthesis, Morphology, Spectral Characterization and Thermal Behaviors of Transition Metal Complexes Containing Oxime-Imine Group," *Erzincan University Journal of Science and Technology*, vol. 13, no. 3, pp. 1263-1270, 2020.
- [23] A. G. A. Maged and A. A. Fayad, "Synthesis and Spectroscopic Characterization of New Heterocyclic Compounds Derivated From 1-(4-aminophenyl)ethan-1-one Oxime as a Starting Material With Evaluate Their Biological Activity," *Biochem. Cell. Arch.*, vol. 20, no. 2, pp. 5211-5222, 2020.
- [24] H. İlkinen, "Synthesis and Characterization of a Novel Benzimidazole-Oxime Ligand and Its Fe (II), Co (II), Ni (II), Cu (II) and Zn (II) Complexes," *Journal of Scientific Reports-A*, no. 049, pp. 1-11, 2022.
- [25] N. J. Hussien, J. M. S. Alshaw, K. T. Abdullah, E. I. Yousif, and M. J. Al-Jeboor, "Dimethyltin (IV) Complexes of New Thiosemicarbazone Ligand With Piperazine-1-ylmethylene Moiety: Synthesis, Spectral Characterization and Antibacterial Activity," *Edelweiss Applied Science and Technology*, vol. 9, no. 3, pp. 266-278, 2025.
- [26] K. T. Abdullah, A. S. M. Al-Janabi, N. J. Hussien, T. A. Yousef, S. Shaaban, M. I. Attia, and O. K. Al Duaij, "Spectroscopic and Biological Studies of Pd(II) Complexes of 5-(p-Tolyl)-1,3,4-oxadiazole-2-thiol," *Bull. Chem. Soc. Ethiop.*, vol. 39, no. 1, pp. 79-90, 2025.
- [27] S. Sengupta, S. Khan, S. K. Chattopadhyay, I. Banerjee, T. K. Panda, and S. Naskar, "Trinuclear Copper and Mononuclear Nickel Complexes of Oxime Containing Schiff Bases: Single Crystal X-Ray Structure, Catecholase and Phenoxazinone Synthase Activity, Catalytic Study for the Homocoupling of Benzyl Amines," *Polyhedron*, vol. 182, p. 114512, 2020.
- [28] P. Kumar Yadav, R. Badekar, K. P. Jain, and R. Lokhande, "Synthesis and Characterization of Co (II), Ni (II) and Cu (II) Complexes With 2-[(4-Bromobenzylidene)hydrazinylidene]-1,2-diphenylethanamine," *Journal of Advanced Scientific Research*, vol. 12, no. 01 Suppl. 1, pp. 287-294, 2021.
- [29] R. S. Bendre, R. D. Patil, P. N. Patil, H. M. Patel, and R. S. Sancheti, "Synthesis and Characterization of New Schiff-Bases as Methicillin Resistant Staphylococcus aureus (MRSA) Inhibitors," *Journal of Molecular Structure*, vol. 1252, p. 132152, 2022.
- [30] S. Slassi, M. Aarjane, and A. Amine, "Synthesis, Spectroscopic Characterization (FT-IR, NMR, UV-Vis), DFT Study, Antibacterial and Antioxidant In Vitro Investigations of 4,6-Bis((E)-1-((3-(1H-imidazol-1-yl)propyl)imino)ethyl)benzene-1,3-diol," *Journal of Molecular Structure*, vol. 1255, p. 132457, 2022.